

Beam dynamics studies on the 100 MeV/100 kW electron linear accelerator for NSC KIPT neutron source

PEI Shi-Lun(裴士伦)^{1,1)} CHI Yun-Long(池云龙)¹ WANG Shu-Hong(王书鸿)¹
PEI Guo-Xi(裴国玺)¹ ZHOU Zu-Sheng(周祖圣)¹ HOU Mi(侯汨)¹ Mykola Ayzatskiy²
Ivan Karnaukhov² Volodymyr Kushnir² Viktor Mytrochenko² Andrey Zelinsky²

¹ Institute of High Energy Physics, Chinese Academy of Sciences, Beijing 100049, China

² Kharkov Institute of Physics and Technology, National Science Center, Kharkov 61108, Ukraine

Abstract: We designed a 100 MeV/100 kW electron linear accelerator for NSC KIPT, which will be used to drive a neutron source on the basis of subcritical assembly. Beam dynamics studies have been conducted to reach the design requirements ($E=100$ MeV, $P=100$ kW, $dE/E < 1\%$ for 99% particles). In this paper, we will present the progress of the design and the dynamic simulation results. For high intensity and long beam pulse linear accelerators, the BBU effect is one big issue; special care has been taken in the accelerating structure design. To satisfy the energy spread requirement at the linac exit, the particles with large energy difference from the synchronous particle should be eliminated at a low energy stage to ease the design of the collimation system and radiation shielding. A dispersion free chicane with 4 bending magnets is introduced downstream of the 1st accelerating section; the unwanted particles will be collimated there.

Key words: beam dynamics, linear accelerator, BBU, collimation system, neutron source

PACS: 29.20.Ej, 29.25.Dz, 29.27.Bd **DOI:** 10.1088/1674-1137/36/7/015

1 Introduction

In the NSC KIPT (National Science Center, Kharkov Institute of Physics and Technology, Ukraine), a neutron source based on a subcritical assembly driven by a 100 MeV/100 kW electron linac will be constructed. This neutron source is an ANL (Argonne National Laboratory, USA) and NSC KIPT Joint project [1], and the linac will be designed and constructed by IHEP, P. R., China. The design and construction of such a linac with a high average beam current, low emittance and low beam power loss is a challenging technical task. Table 1 shows the main specifications of the linac.

2 Linac layout

For high intensity electron linacs, both the regenerative and cumulative beam break-up (BBU) effects

need to be considered. In our design, the following measures are employed to suppress the BBU effects.

Table 1. Main specifications of the NSC KIPT linac.

parameters	values
RF frequency/MHz	2856
beam energy/MeV	100
beam current (max.)/A	0.60
energy spread (1σ)(%)	1
emittance (1σ)/(m-rad)	5×10^{-7}
beam pulse duration/ μ s	2.7
gun high voltage/kV	120
accelerating structure	10 units/1.336 m
klystron	6 units/(30 MW/50 kW)
RF pulse width/ μ s	3.0
RF repetition rate (max.)/Hz	625

1) Using a short quasi-constant gradient accelerating structure (~ 1.35 m long) to spread the dipole higher order mode (HOM) frequencies along the structure.

Received 26 August 2011

1) E-mail: peisl@mail.ihep.ac.cn

©2012 Chinese Physical Society and the Institute of High Energy Physics of the Chinese Academy of Sciences and the Institute of Modern Physics of the Chinese Academy of Sciences and IOP Publishing Ltd

2) Applying a solenoid magnetic field along the 1st accelerating structure.

3) Increasing the accelerating gradients of the 1st and 2nd accelerating structures to enhance the beam energy boosting rate at the low energy stage as much as possible.

4) Decreasing the pulsed beam current to 0.6 A and the beam pulse length to 2.7 μs .

5) Introducing triplet quadrupoles downstream of every one or every two accelerating structures.

6) Adopting a better alignment with an accuracy of less than 0.2 mm (1σ).

7) Employing the beam orbit correctors to control the beam orbit as close to the accelerating structures' axes as possible.

Figure 1 shows the schematic layout of the whole linac. 6 klystrons and 10 accelerating sections are employed with a total dynamical length of ~ 22.3 m from the electron gun exit to the linac end. ~ 10 kW and $\sim 2\text{--}3$ MW input RF power are needed for the pre-buncher and buncher, while 16 MW and 20 MW power for the 1st and 2nd accelerating structures (A0-A1), 10 MW input power is needed for each of the rest of the accelerating structures (A2-A9). A dispersion free chicane system located downstream of the 1st accelerating section was designed to collimate the particles with a large energy difference from the synchronous particle; in this way the total beam power loss along the whole linac can be minimized.

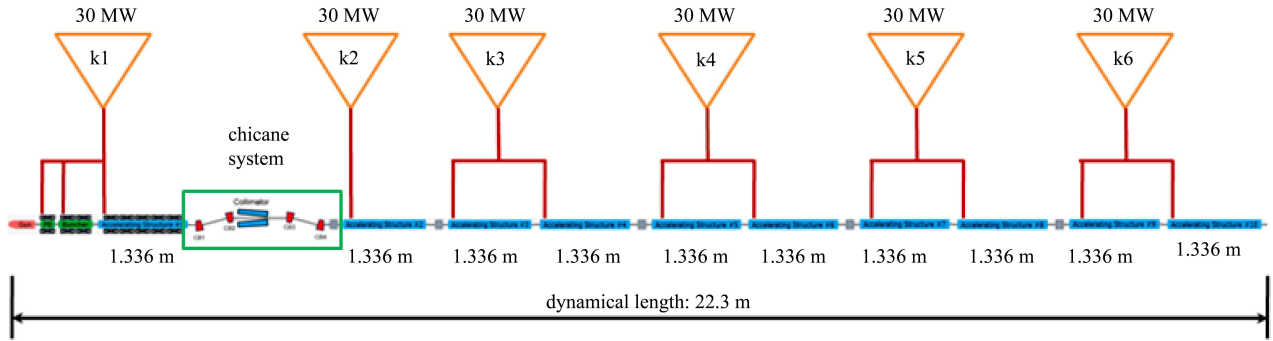


Fig. 1. The schematic layout of the NSC KIPT linac.

3 Accelerating structure design

10 accelerating structures are employed to boost the beam energy to 100 MeV. Table 2 shows the main parameters of the accelerating structure. To suppress the BBU (both regenerative and cumulative) effects, a ~ 1.35 m long $2\pi/3$ mode quasi-constant gradient structure was adopted. The disk hole diameter decreases from 27.887 mm to 23.726 mm in a stepwise fashion along the structure (26.220 mm to 19.093 mm for SLAC type 3 m long structure). To detune the dipole higher order modes quickly, the dipole mode frequency spread was increased by increasing the average disk hole diameter step to ~ 0.122 mm (~ 0.085 mm for the SLAC type 3 m long structure). At the 3rd to 6th disks of each structure, 11 mm diameter holes will be drilled, by which the frequency of the HEM11 mode can be increased from ~ 4042 MHz to ~ 4050 MHz.

Due to the high averaged RF power loss in the linac structure, water jacket cooling is needed to sufficiently cool down the structure. Using the multi-

physics software package ANSYS [2], numerical RF-thermal-structural-RF coupled finite element analysis (FEA) on the accelerating structure has been carried out [3]. The cooling water flow rate is finalized at 10 t/h.

Table 2. Accelerating structure parameters.

parameters	values
operation frequency/MHz	2856
operation temperature/ $^{\circ}\text{C}$	40.0 ± 0.2
number of cells	34 regular cells 2 coupler cells
section length/mm	1260 (36 cells)
phase advance per cell	$2\pi/3$
cell length/mm	34.989783
disk thickness (t)/mm	5.84
iris diameter ($2a$)/mm	27.887–23.726
cell diameter ($2b$)/mm	83.968–82.776
shunt impedance (r_0)/(M Ω /m)	51.514–57.052
Q factor	13806–13753
group velocity (v_g/c)	0.02473–0.01415
filling time/ns	215
attenuation parameter/Np	0.1406

4 Beam dynamics

EGUN [4] and PARMELA [5] were used for the beam dynamics study. Starting with the beam parameters at the gun exit calculated with EGUN, a 100 kV/0.85 A/3.85 ns/3.27 nC electron beam was used as an input of PARMELA to simulate and optimize the beam performance at the linac exit. 10000 initial particles were used. Fig. 2 shows the beam optics in the electron gun. An electron beam with a normalized emittance of 5.264 mm-mrad can be obtained at the gun exit.

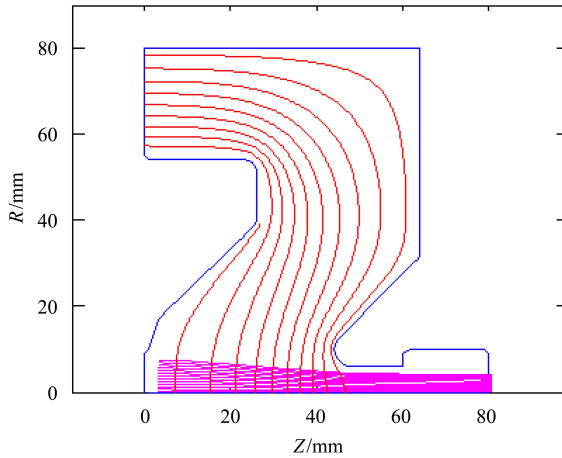


Fig. 2. The beam optics in the electron gun for the 0.85 A/100 kV beam.

The bunching system we normally used has a transportation efficiency of ~85%. According to our

simulation, there will be ~15% particles downstream of the 1st accelerating structure which cannot meet the 1% (1σ) energy spread requirement for 99% of particles at the linac exit, and they should be eliminated at the low energy stage by a chicane system. The beam collimator is located between the 2nd and 3rd bending magnets (where there is the largest dispersion) to collimate the particles with a large energy spread. Conclusively, the linac would have ~70% transportation efficiency (from the gun exit to the linac end). To get a better beam performance, the chicane system was designed to be dispersion free by optimizing the edge angles of CB2 and CB3. After passing through the chicane system, the bunch length will be increased by ~4.2%, and ~2 kW beam power will be lost in the collimator.

The beam collimation process is shown in Fig. 3. The left 4 plots are at the CB1 entrance and the right 4 ones are at the CB4 exit. Here the phase spectrum, beam profile, energy-phase distribution and energy spread are shown. It can be seen from the energy-phase distribution that the particles with a large energy difference from the synchronous particle are collimated successfully.

Figure 4 shows the beam bunching process, in which the longitudinal beam performance (phase spread and beam energy spread) at 5 locations (the gun exit, the pre-buncher exit, the buncher entrance, the buncher exit and the 1st structure A0 exit) are shown, respectively. The beam is transversely focused by ~25 solenoids from the gun exit to the A0 exit.

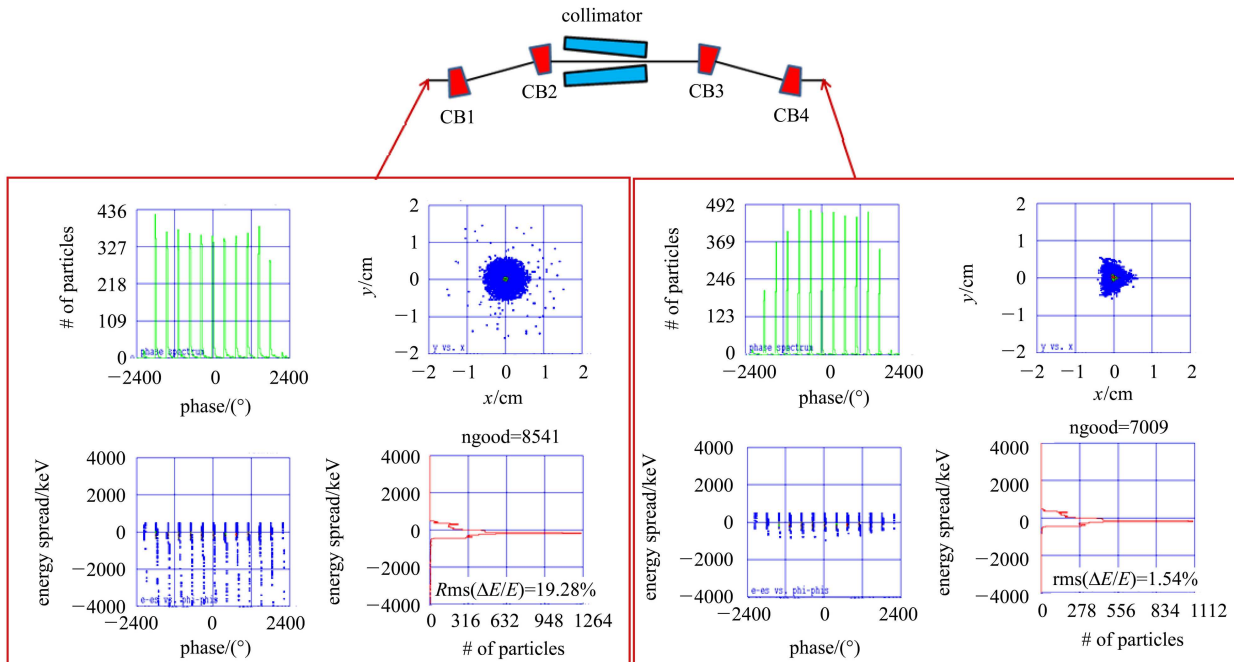


Fig. 3. The beam collimation process.

Figure 5 shows the transverse beam envelopes along the whole linac. Fig. 6 shows the PARMELA simulation results of the phase spectrum, the beam size, the energy spectrum and the energy spread from the upper left to the lower right at the linac end. It can be seen that the energy spread is 0.65% for 6933 good particles (99% of the total 7009 good particles at the linac end). The simulated 1σ normalized emit-

tance by PARMELA in two transverse directions is 23.4 mm·mrad and 23.9 mm·mrad (fairly lower than the design requirement) respectively without any error effects being considered. Even when the error effects (beam alignment, transverse wakefield, beam phase, etc) were considered, the total rms normalized emittance would be lower than the design requirement of 100 mm·mrad.

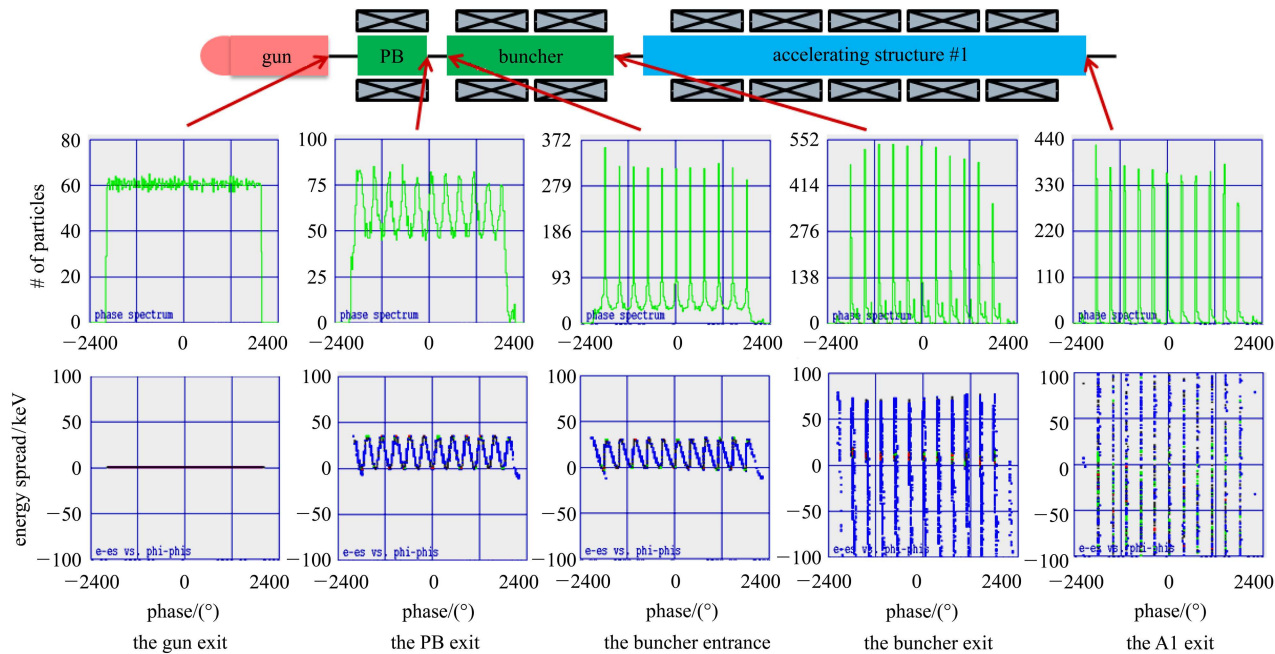


Fig. 4. The beam bunching process.

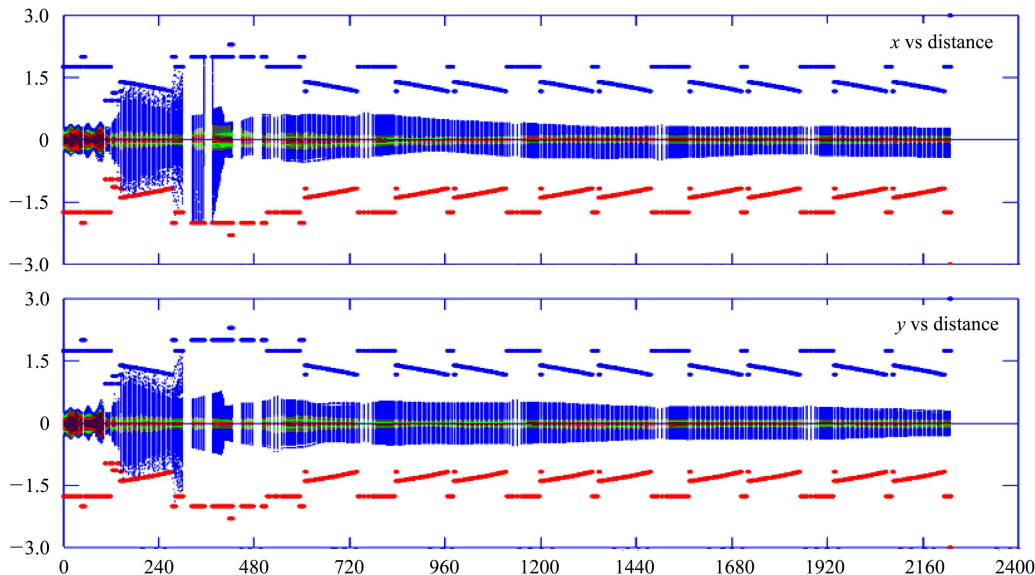


Fig. 5. The beam envelopes along the whole linac (unit:cm).

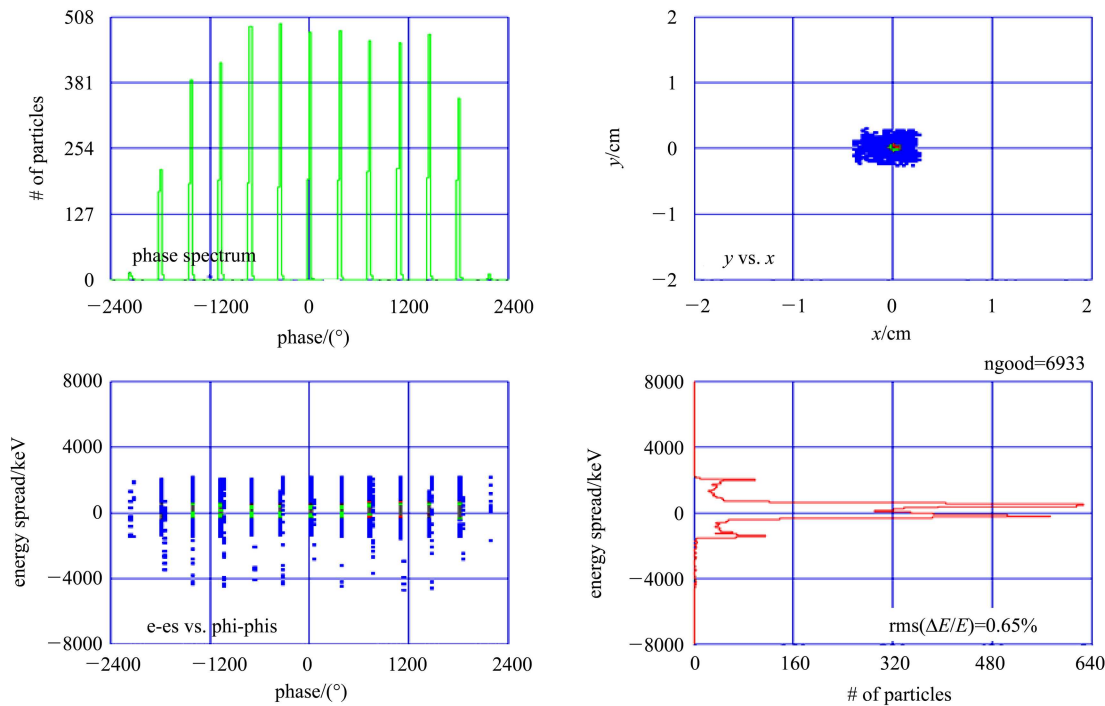


Fig. 6. The PARMELA simulation results at the linac end.

5 BBU effects

The BBU calculation methodology is shown in Fig. 7. For each accelerating cell, dipole modes of the 1st six dipole bands were calculated by MAFIA [6]. Figs. 8 and 9 show the synchronized dipole modes' kick factor and quality factor. For the ~ 1.35 m long structure, ~ 216 dipole modes were considered. Here, no solenoid magnetic field was applied, which is very helpful for BBU suppression at low energy stage. In the simulations, the cases with or without beam orbit corrections were considered.

Figure 10 shows the beam offset and angle distribution caused by the dipole modes of one $0.85 \text{ A} / 2.7 \mu\text{s}$ electron beam along the 1st accelerating structure. The left plot is for no orbit correction case, while the right one is for the orbit correction case. Here, $+300 \mu\text{m}$ and $+300 \mu\text{rad}$ initial beam offset and trajectory angle, which can cause the largest beam offset than the other combinations of initial offset and angle, were assumed. It can be seen that the largest beam offset caused by the dipole modes in the 1st accelerating structure is $\sim 0.8 \text{ mm}$ without beam orbit correction and $\sim 0.36 \text{ mm}$ with correction.

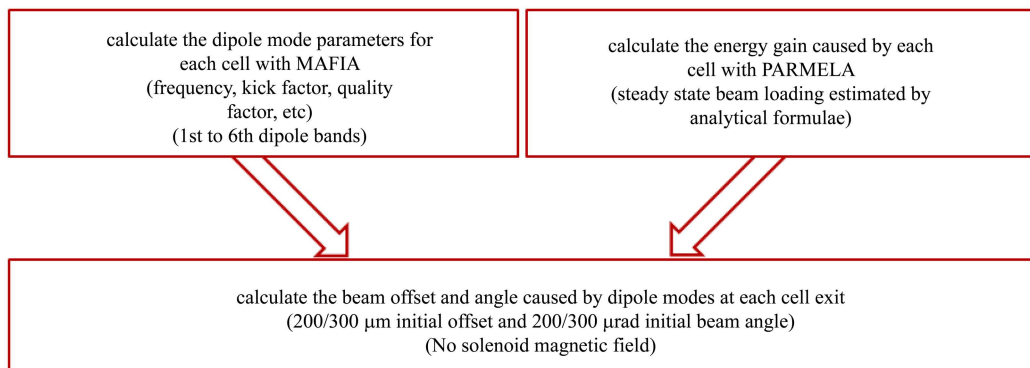


Fig. 7. The BBU calculation methodology.

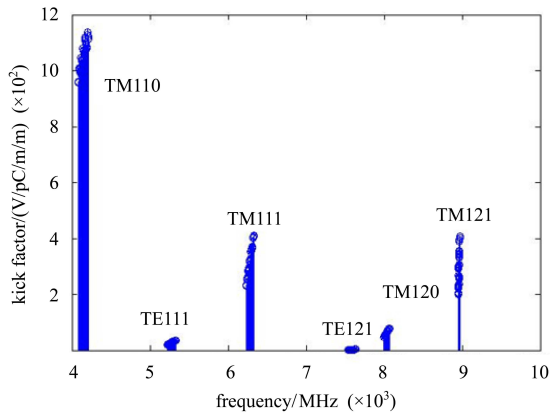


Fig. 8. The synchronized dipole modes' kick factor.

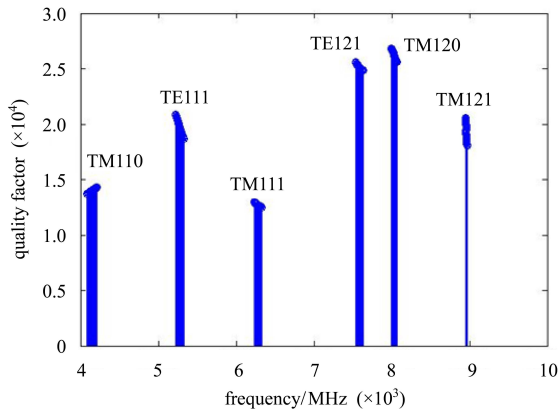


Fig. 9. The synchronized dipole modes' quality factor.

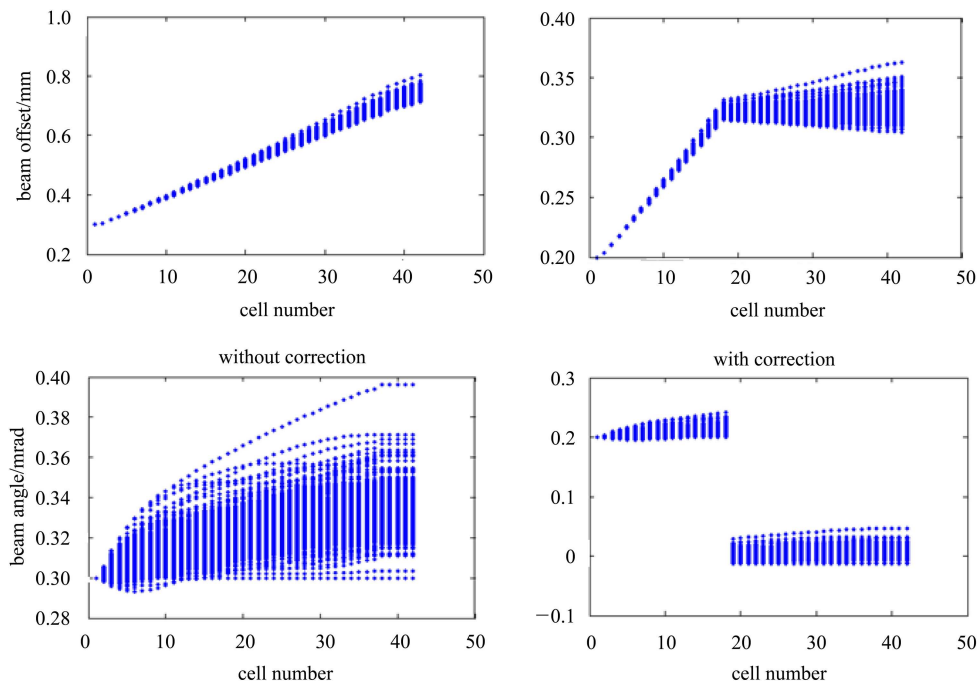


Fig. 10. The beam offset and angle distributions along the 1st 1.35 m long accelerating structure.

Figures 11 and 12 show the cumulative BBU effect calculation results. The two left plots are for the no orbit correction case, while the two right two ones are for the orbit correction case. Here in Fig. 11, the $+200 \mu\text{m}/+200 \mu\text{rad}$ ($+300 \mu\text{m}/+300 \mu\text{rad}$ for Fig. 12) initial beam offset and angle are assumed for the upper two plots, while $+200 \mu\text{m}/-200 \mu\text{rad}$ ($+300 \mu\text{m}/-300 \mu\text{rad}$ for Fig. 12) is assumed for the lower two ones. If the largest beam offset is compared with the aperture of the accelerating structure, it can be clearly seen that the beam can successfully go through the linac by adopting a better alignment with an accuracy of less than 0.2 mm (1σ) and with beam orbit correction.

6 Beam power loss

The beam loss simulation is done with PARMELA. Fig. 13 shows the result. Most of the beam power loss is located at the chicane region, where the electron beam has a relatively large energy spread and $\sim 1.7 \text{ kW}$ of beam power are collimated by the collimator. The total beam power loss along the linac (from the gun exit to the linac end) is $\sim 2 \text{ kW}$, about 2% of the total beam power at the linac exit.

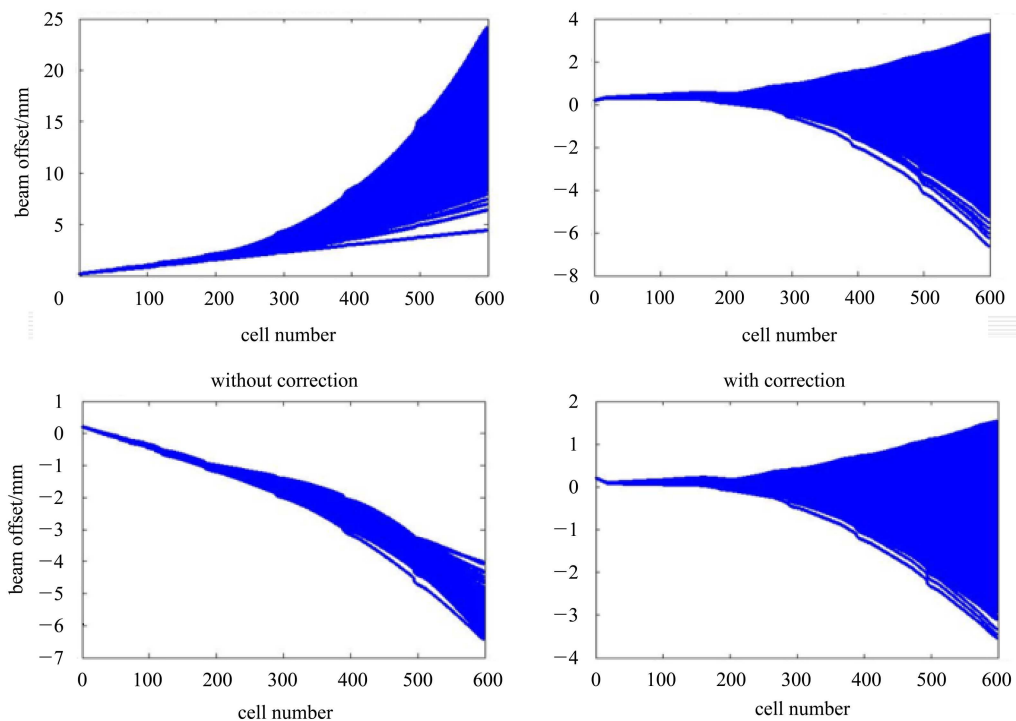


Fig. 11. The beam offset distribution of one 0.85 A/2.7 μs beam along the whole linac with +200 μm/+200 μrad (the upper two plots) and +200 μm/-200 μrad (the lower two plots) initial offsets and trajectory angles.

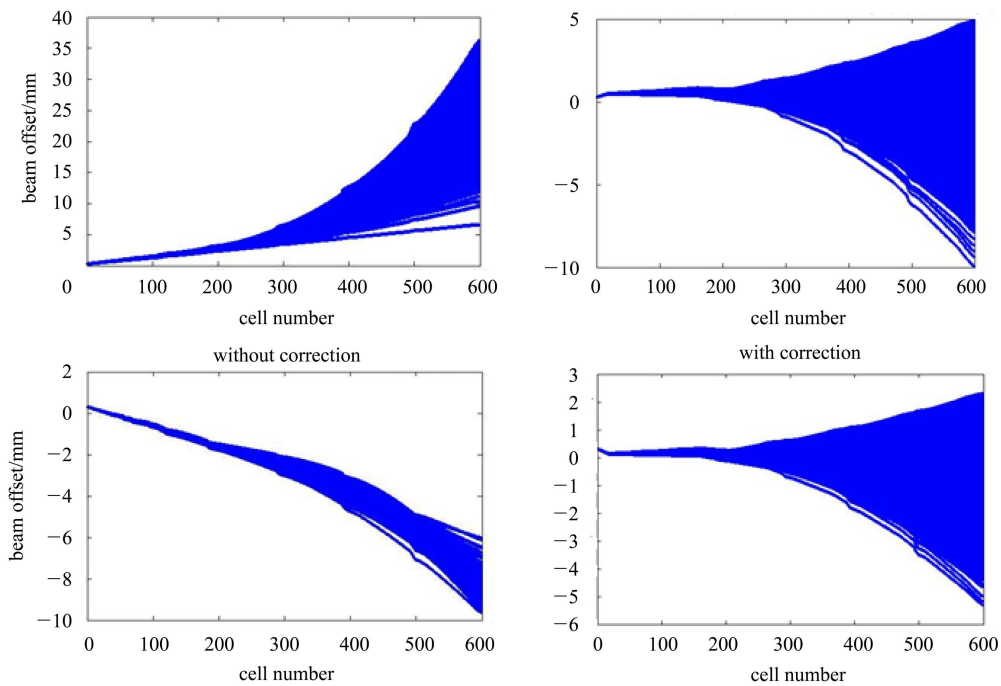


Fig. 12. The beam offset distribution of one 0.85 A/2.7 μs beam along the whole linac with +300 μm/+300 μrad (the upper two plots) and +300 μm/-300 μrad (the lower two plots) initial offsets and trajectory angles.

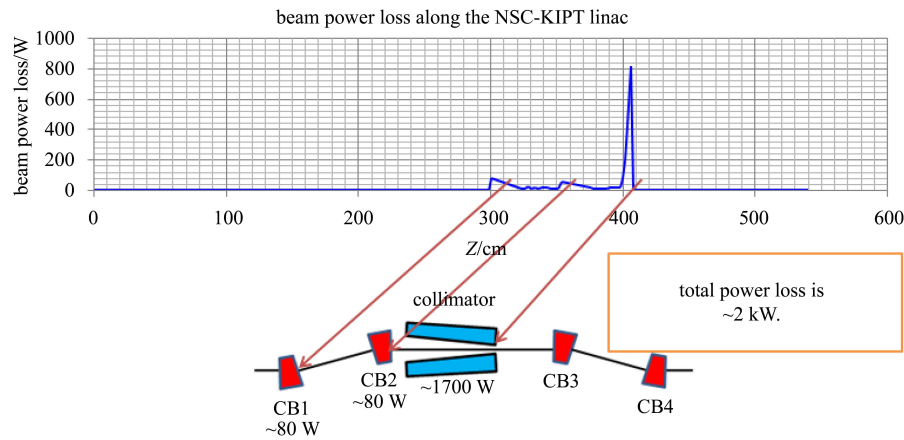


Fig. 13. The beam power loss distribution along the linac.

7 Summary

One 100 MeV/100 kW electron linear accelerator is to be constructed at NSC KIPT and will be used to drive a neutron source on the basis of subcritical assembly. The beam dynamics design has been

done with EGUN and PARMELA. BBU studies have been carried out. To suppress the beam power loss at the high energy stage and to facilitate the radiation shielding system, a dispersion free chicane with 4 bending magnets was designed for the purpose of beam collimation. The simulation results show that our design is good enough to satisfy the design requirements.

References

- 1 CHI Yun-Long et al. Design Report on the NSC KIPT Electron Linear Accelerator. Version 2, IHEP, 2011.8
- 2 ANSYS is a Trademark of SAS Inc. www.ansys.com
- 3 PEI Shi-Lun et al. RF-Thermal-Structural-RF Coupled Analysis on the Travelling Wave Disk-loaded Accelerating Structure. Chin. Phys. C (HEP & NP), 2012, **36**(6): 555–560
- 4 Herrmannsfeldt W B. Egun-An Electron Optics and Gun Design Program. SLAC-331, UC-28, (A), 1998.10
- 5 Young L M et al. Parmela. LA-UR-96-1835. Los Alamos National Laboratory, Revised July 19, 2005
- 6 The MAFIA collaboration. MAFIA User Manual version 4.106. Germany: CST Inc., 2000